1978

Comparison of Mathematical and Experimental Simulation of Lubrication Conditions in the System Of Piston, Piston Ring and Liner

F. Wrede

COMPARISON OF MATHEMATICAL AND EXPERIMENTAL SIMULATION OF LUBRICATION CONDITIONS IN THE SYSTEM OF PISTON, PISTON RING AND LINER

F. WREDE, Dipl.-Ing.
wiss. Assistent

Technical University of Hannover / Germany

INTRODUCTION

The system of piston, piston ring and cylinder represents the most important assembly for transmitting forces in the reciprocating piston compressor. The sliding motion of the piston is very complex because of simultaneous oscillating and transversal tilting. Owing to the resulting frictional process the periodical energy conversion in the working chamber is dissipative. Furthermore this assembly works as a tribological system. Therefore in lubricated compressors it is the aim to separate the sliding surfaces by a hydrodynamic lubrication film. This is only possible by preventive measures in the construction of the interacting elements concerning makro and mikro geometry and also supplying lubricant.

In this sense the theory of hydrodynamic lubrication represents an essential tool in design practice. Owing to the difficult physical interactions it took a long time for introducing this method. But until now a lot of papers concerning this special problem have been published. Many different mathematical models have been presented and for that reason a need for experimental verification of theoretical results is obvious.

ANALYSIS

Continuing the treatises of Kruse /1 - 3/ and Burmeister /4/ the assembly of piston, piston ring and liner is considered as an interacting unit. For preventing immediate solid or even boundary friction both have to slide on a common fluid film. Postulating the well-known assumptions for incompressible Newtonian fluid lubrication the mathematical problem may be described by the general Reynolds differential equation.

$$\frac{\partial}{\partial x}\left(h^3 \frac{\partial p}{\partial x}\right) + \frac{\partial}{\partial z}\left(h^3 \frac{\partial p}{\partial z}\right) = 6\eta(U_1 - U_2)\frac{\partial h}{\partial x} + 6\eta h \frac{\partial}{\partial x}(U_1 + U_2) + 12\eta V \tag{1}$$

The second right hand term describes the so called stretch effect which in general is not of importance.

Both analytical and numerical methods exist to calculate the lubrication conditions. The premise for an analytical solution is to neglect the circumferential flow given by the second left hand term. The resulting two dimensional expression

$$\frac{\partial}{\partial x}\left(h^3 \frac{\partial p}{\partial x}\right) = 6\eta U \frac{\partial h}{\partial x} + 12\eta V \tag{2}$$

reproduces the instationary case including variable speed and squeeze effect. A further simplification yields an equation for steady state conditions neglecting also squeeze effect and assuming constant speed.

$$\frac{\partial}{\partial x}\left(h^3 \frac{\partial p}{\partial x}\right) = 6\eta U \frac{\partial h}{\partial x} \tag{3}$$

The analytical treatment of this equation considering piston, piston ring and liner as a unit was given by Kruse /1-3/. Figure 1 shows the corresponding geometry of the sliding element assuming a double wedge type piston ring profile. The solution of this analysis contains only simple algebraic expressions /3/ for the load capacity

$$F_P = \int_0^A p_y \, d_x \, d_z \tag{4}$$

and the frictional force

$$F_R = \int_0^A \tau_{yx} \, d_x \, d_z \tag{5}$$

also already represented to the 1974 Purdue Conference.

Even the most simple threedimensional set of Reynolds equation for steady state conditions must be solved by a numerical procedure.

$$\frac{\partial}{\partial x}\left(h^3\frac{\partial p}{\partial x}\right)+\frac{\partial}{\partial z}\left(h^3\frac{\partial p}{\partial z}\right)=6\eta U\frac{\partial h}{\partial x} \tag{6}$$

The euqation has to be transformed into a system of finite difference expressions. Burmeister /4/ first used this method including an overrelaxation procedure for numerical treatment. Later on Das /5/ used the same technique for cyclic calculating of lubrication conditions basing on the equation

$$\frac{\partial}{\partial x}\left(h^3\frac{\partial p}{\partial x}\right)+\frac{\partial}{\partial z}\left(h^3\frac{\partial p}{\partial z}\right)=6\eta\left(2V+U\frac{\partial h}{\partial x}\right) \tag{7}$$

This author did not succeed in completing the cyclic calculation even over a greater part of the piston path not to mention over the whole stroke. The reasons are given in the extensive calculating effort overcharging also very efficient computers.

In comparing the results of computations based on the two- and on the three-dimensional mathematical model for steady state conditions Burmeister /4/ stated very small differences. Both lubricating film forces and film thickness experienced deviations in the order of of 1 %. Because of the important possibility of mathematical simulation for parameter studies in a wide range not to be performed in experimental research, it is worthwile to compare also mathematical and experimental results to check the simulation model and its boundary conditions.

EXPERIMENTAL RIG FOR THE SIMULATION OF PISTON AND PISTON RING LUBRICATION

Since 1925, when Stanton /6/ started to investigate cylinder lubrication, a lot of experimental research was carried out to reproduce the mechanism of lubrication and wear concerning piston, piston ring and liner. The experience showed the great difficulty to explore lubrication in such an inaccessible system. The development led to glasscylinder engines, special apparatus with cylindrical geometry and to plain slider bearing systems. With the refinement of measurement and instrumentation technique it became possible to obtain some transparency in this problem.

(1) General Requirements for a Model Type Experimental Rig

The lubrication conditions in a hydrodynamic slider bearing are characterized by the following primary or secondary measurable variables:

- oil film pressure
- oil film temperature
- oil film thickness

These are so-called main process variables.

The first and second are of special importance. The correlation between calculation and experiment will be optimally tested by verification of the theoretical assumed /1/ significant pressure profile, Figure 2, and consequently entirely indicated hydrodynamic conditions.

A direct measurement of the oil film temperature is hardly possible up to now. From the experiments by Stribeck /7/ a systematic method can be deduced to stabilize the dynamic viscosity isothermal and to measure the surface temperatures of the lubricating gap.

The gauging of the oil film thickness is corresponding to mathematical results to be done in that way, that roughness and waviness of surfaces are eliminated. For this purpose at least at the beginning of experiment surfaces should have a mathematical ideal finish.

For the derivation of similarity principles additional directions should be preservered

- geometric similarity of model and master type
- oscillating relative motion between piston and liner
- variable cinematics of the crank assembly
- variable lubricant supply
- direct measurement of the lubricating film forces.

The last condition can be realized very simply by dynamometric suspension of the model type piston combined with an oscillating liner. A further advantage can be achieved, if besides realistic oscillating and variable motion also steady state conditions with constant velocity are possible. But the most important requirement is to measure all main process variables simultaneously.

(2) The Characteristic Coefficients of the Model

As following described in contrary to the experiments of Brown and Hamilton /8/ the geometry of the system piston, piston ring and liner is dimensioned as large as possible. The reason is , to use controllable measurement technique and to get transparency by large scale. The geometric similarity is given by adhering to a constant scale factor for all corresponding dimension sizes. The running profile of the piston ring is defined by the coefficient of shape.

$$FK=\frac{\Delta h\cdot RL}{C^2} \tag{8}$$

It contains all characteristic dimensions for the load capacity of the profile besides the ring length RL the edge chamfer Δh and the length C of the middle land. The dimensions of the ring profile are given in Figure 3. The flow of the incompressible lubricant in the gap is to be mechanically similar under the exclusive action of frictional forces. The physical similarity of the flow demands besides geometrical similar definition of the lubricating gap also geometrical similar configuration of flow. By introducting dimensionless coefficients in the equations of motion or with the help of the π-theorem the Reynolds law of similarity /9/ can be deduced. According to that flows at geometrical similar bodies are dynamically similar if the Reynolds numbers described by the equation

$$Re = \frac{U \cdot c_{min}}{\nu} \qquad (9)$$

are identical.

The characteristic dimension of the lubricating gap is described by the thickness of the fluid film c_{min}. By appropriate choice of the relative speed U or of the kinematic viscosity ν the postulation of similarity can be maintained. As the quotient of mass and frictional forces the Reynolds number is a characteristic value for the control of inertia forces in the flow. Kahlert /10/ introduces a coefficient similar to the Reynolds number

$$Re^{*} = \frac{U \cdot RL}{\nu} \left(\frac{c_{min}}{l} \right)^2 \qquad (10)$$

which is especially suitable for the conditions concerning piston rings.

The dimensional analysis concerning Reynolds differential equation carried out by Ryk and Rogov /11/ yields four dimensionless coefficients

$$P_1 = \frac{y}{x} \qquad (11)$$

$$P_2 = \frac{z}{x} \qquad (12)$$

$$P_3 = \frac{U}{V} \qquad (13)$$

$$P_4 = \frac{x \cdot p}{\eta \cdot U} \qquad (14)$$

These criteria of similarity are on the one hand parameter quotients of the geometry, P_1 and P_2, which are to be preserved by the scale factor of model and master type. An additional so-called similarity simplex P_3 describes the relation between the relative translatory velocity and the transversal velocity $v = \delta h/\delta t$. Finally a similarity complex P_4 results which represents the complete laws of similarity for transformation of the concerned fundamental dimensions. This coefficient composed of the pressure p and the axial length x the dynamic viscosity η and the relative velocity U corresponds to the Sommerfeld number characterizing the load conditions of a journal bearing.

$$So = \frac{\bar{p} \cdot \psi^2}{\eta \cdot \omega} \qquad (15)$$

Here it is modified for the piston ring to

$$So^{*} = \frac{p_N \cdot RL}{\eta \cdot U} \cdot FK \qquad (16)$$

so that this coefficient can describe the specific load and the geometry.

(3) General Lay Out of the Experimental Rig

Figure 4 shows a survey drawing of the experimental rig. The plane sliding system and the drive are arranged on a common plate. The sliding system of piston, piston ring and liner consists of the plane piston model and a band-shaped piston ring as well as the plane liner on a support with linear roller bearing. The main dimensions of this apparatus are derived regarding the above given dimensions. It was the intention to realize a quasi infinite width. Concerning the above mentioned main process values the pressure profile in the lubricating system is of greatest importance. As it is not possible to construct a punctiform pressure pick up for gauging this pressure profile certain relation between the diameter of the pick up and the axial height of the piston ring as one main dimension of the pressure profile is to be kept. Concerning the measurment technique as chosen here to measure the pressure profile by a thin tube as sampling device with a diameter of 0,2 mm Ø and a piezoelectric pressure gauge an axial height of the piston ring of 10 mm is necessary. According to standard values of Englisch /12/ and Neale /13/ a piston diameter of D = 500 ./. 600 mm corresponds to this dimension. Thus the piston stroke of such an engine is given. By constructional means in the model a stroke of s = 800 mm was realized. The time behaviour of the provided gauges allows a maximum relative velocity of piston and liner in the order of v = 4,5 m/s.

The latitude of the sliding system was defined by a mathematical simulation. As result Figure 5 shows the development of pressure as a function of the latitude of the sliding system. With an increase of latitude the pressure level approximates the boundary value of an infinite wide slider. In the near of 150 mm width of the bearing the pressure deviates in the order of 2 % from the limiting value. For financial and constructing reasons a slider width of 160 mm was realized.

(4) Description of the Slider Model

Figure 6 shows the really important component parts of the rig. These are the plane piston, the band shaped piston ring, the liner, the nozzle duct for oil supply and the several gauges. The running profile of the piston ring, Figure 3, was produced by grinding on a surface grinding machine. The angles of the flanks are dimensioned corresponding to the statements in literature /13, 14/ for broken in piston rings. These found in literature are in the order of $0{,}1^{0}$ - $0{,}8^{0}$. To simulate the elastic pressure of the piston ring, expressed by the piston rings tangential force a flat leaf spring is installed. This spring is of the same shape as used in Wankel type engines. The elastic pressure derives from

$$p_E = \frac{2 \cdot F_t}{d \cdot h_1} \qquad (17)$$

the tangential force and the cross sections geometry of the actual piston ring. In the model it is simulated in the same order and moreover can be intensified for loading the lubrication film. The surfaces of the sliding configuration are superfine grinded and of extreme planeness. In contrary to the real piston-type machine the model needs a special oil supply. The oil splash lubrication in this case is substituted by a nozzle duct. A speed governed geared pump feeds the distributor with six single nozzles. The amount of oil can be governed from 0,1 - 1,0 l/min and supplies the system from the one and very side according to the pistons bottom side of the real-type machine.

(5) The Drive System of the Rig

In the model rig the crank assembly is substituted by a hydrostatic linear drive. It consists of a hydraulic circuit, a double-acting high speed hydraulic cylinder, an electro-hydraulic servo valve and an electronic crank assembly simulator, Figure 7. In the real-type machine the components piston, connecting rod and crankshaft couple the oscillating translatory motion of the piston according to the laws of crankshaft assembly kinematics:

stroke-connecting-rod ratio

$$\lambda = r / l \qquad (18)$$

piston path

$$x_s = r\left[1 - \cos\omega t + 1/4\,\lambda\,(1 - \cos 2\omega t)\right] \qquad (19)$$

piston velocity

$$v_s = r\omega(\sin\omega t + \lambda/2 \sin 2\omega t) \qquad (20)$$

piston acceleration

$$a_s = r\omega^2(\cos\omega t + \lambda \cos 2\omega t) \qquad (21)$$

The electronic crankshaft assembly simulator, Figure 8, allows variations in the following range

$r = 0 - 400$ mm

$\lambda = 0 - 0{,}3$ -

$\omega = 0 - 12\ s^{-1}$

and also to drive with constant speed from 0 - 4,5 m/s over 1/3 - 1/2 of the stroke.

(6) The Measuring Devices

The theory of hydrodynamic lubrication represented in the mathematical simulation models for the piston, piston ring and liner unit demands the verification by measuring the interacting pressure profile. For this task a miniature pressure pick-up combined with a needle adapter was installed into the piston liner. Figure 9 shows the installation of the pressure gauge surrounded by thermo couples for measurement of the surface temperature. The time and transmission behaviour of the adapter system was tested theoretically by the method of Elson and Soedel /15/ and in experiment by feeding with pressure impulses. A sufficient recording exactness was proved by both methods including frequency analysis of the real pressure signal which is similar to a transient half sine-shaped pressure impulse.

The mathematical reproduction of the sliding mechanism is based on exact knowledge of the lubrication gap geometry. The minimum thickness of the lubricating film is especially important as well as the clearance between piston and liner. In the experiments given by literature alternatively capacitive and inductive gauges are used. Both methods show special problems. The capacitive measuring principle is strongly influenced by the properties of the dielectric for instance an unknown oil gas mixture. The inductive gauges need exact temperature compensation.

In the experiments described here stabilized temperature conditions are aimed. Under this point of view inductive gauges seemed to be advantageous. Figure 9 and Figure 10 show the installation of the distance gauges in the liner and the piston ring. The pick-ups observing the piston clearance are to be seen from Figure 6.

As well-known the viscosity of lubricant in the gap is strongly dependant from the temperature. A direct measurement of temperature within the lubrication film is also in the model of piston, piston ring and liner not exactly possible. Therefore the surface temperatures of the sliding components are measured for deducing the effective viscosity in the lubricant like in the experiments of Wing and Saunders /16/. At all parts 2 x 0,3 Cu-Ko thermo-couples are applicated. These thermo-couples are of extremely small dimensions and have a stable calibration curve.

The pressure profile in the lubrication film generates during the motion of the slinding parts load capacity and frictional forces. To measure these lubricant film forces the piston model is suspended by a prestressed three-component dynamometer, Figure 6.

For controlling the variation of kinematic conditions also the stroke, the velocity and the acceleration is measured.

PRESENTATION OF RESULTS

In the following the results of mathematical and experimental simulation of the lubrication behaviour under steady state conditions shall be described. Corresponding to the above treated theoretical models the subsequent aspects are of main interest:

- verification of the theoretical pressure profile
- measurement of lubricating film forces
- evaluation of the lubricant supply and distribution
- derivation of similarity coefficients.

For principle experiments measurements concerning a model with a single piston ring are discussed. The variable parameters are:

- relative velocity, loading of the piston ring
- amount of lubricant

Figure 11 shows the three-dimensional pressure profile according to Kruse /1/ which is to be verified at first. The corresponding measured pressure profile in the middle of the sliding system with an accumulation of oil before the leading edge of the piston ring is given in Figure 12. The length of lubricant accumulation filling the piston clearance is equal to the length of the piston ring zone. The linear pressure gradient in the area of the piston is clearly to be seen. This continues with a steep flank in the area of the piston ring and reaches its maximum in the leading wedge. In the area of the middle land of the running profile the pressure subsequently decreases and leads in the extension of the trailing wedge to the boundary level. By this the interactive lubricant film in the unit of piston, piston ring and liner is confirmed. No effect can be stated as for instance disruption or pressure drop of the oil film due to the axial clearance of the ring in its groove. Also there is no equalization of pressure. The assumption of Kruse /1/ that there is the same pressure in the ring groove as in front of the leading ring edge could not be proved under the working conditions of the model. A plausible explanation can be given by the large cross sections between ring and groove which cannot be filled with lubricant under the realized experimental conditions.

By reduction of oil supply the piston ring produces a pressure profile just of its own. Figure 13 shows this case in a computer plot and the corresponding experimental record is given in Figure 14.

From the experiments of Brown and Hamilton /8/ a cavitation phenomenon at the trailing wedge of the piston ring is known. This can also be stated here with the difference in the amplitude of cavitational pressure. It was found to be in the maximum of the order of 0,3 - 0,4 bar under extremely low loading conditions of the fluid film. For example see Figure 15. With higher loading this effect can be neglected.

The Figures 16 a - c show the variation of piston ring loading. The oil supply is quantitatively regulated in that way that there is always a circa 10 mm long oil accumulation before the leading edge of the piston ring. The piston clearance corresponds by scale factor to the standard value. Starting from the standard value of elastic pressure of the piston ring p_E = 0,5 bar the specific loading of the fluid film is increased up to p_E = 5 bar. This upper limit is given preliminarily by constructional reasons because of the ring loading by flat leave springs in the clearance of the ring groove. The maximal value of the pressure profile p_{max} as a criterion for the load capacity of the lubricant film is plotted over the pressurising p_E. In contrary to the following results a relative wide spread of the values compared to the mathematical determined course is to be seen. The reason for this is the not exactly reproducible oil accumulation before the piston ring. By this the level of the whole pressure profile is influenced. With longer accumulation the pressure level and frictional force are higher and with shorter accumulation vice-versa.

Consequently the oil supply was reduced to avoid accumulation and in further measurements lubrication conditions of the piston ring were exclusively tested. The corresponding results are given in Figure 17 and now show a better correlation to the theoretical curves. The first progressive decreasing thickness of the lubrication film is stabilized with increasing load to a linear course. The resulting frictional force corresponds to this tendency. Besides the variation of oil supply and loading different velocities were examined. Figure 18 a - c shows the produced results. With constant load a pressure profile with equivalent load capacity is to be expected. According to figure 18a an insignificant decrease in the maximal pressure p_{max} occurs. A theoretical explanation can be given by figure 19 showing a more massively developed pressure profile.

The mathematical results correponding to those of the experiments are given in figures 16-18 by the straight lines. These are all calculated with the three-dimensional model for simulation of lubrication conditions. The maximal deviation of measurement values are in the order of 10-15%.Concerning the coorrelationship between the results of two and three-dimensional simulation models the following comparison is of importance.

Under same running conditions the maximal values of oil pressure in any case under copious oil supply are greater than without oil accumulation before the ring. The pressure level of the three-dimensional model is always greater then the two-dimensional result. The reasons are boundary effects as pressure drop and transversal flow which are to be compensated in order to reach the same load capacity. Minimum film thickness and frictional forces correspond to theses influences. The deviations of film thickness are in the order of 4-5% related to the maximal values. The frictional forces differ in the same sense as the pressure levels by quantities of circa 3%.

As a summary it can be stated that in a case with an existing transversal flow of significance under length to width ratios of the bearing system from about 1:8 in the maximum the deviations in the order of 1% stated generally by Burmeister /4/ can not be confirmed. Here they are remarkable greater. Concerning piston and piston ring geometry the length to width ratio extends for small pistons from 1:15 to large pistons with 1:50.

Much more important is the calculating effort for both simulation models. The amount of calculating time for the three-dimensional model differs in the average by the factor 2000-3000 to the two-dimensional program.The deviation of both calculating methods for realistic cases of practice are to be estimated straightforward. Therefore the two-dimensional model is a suitable tool for parameter studies intelligibly exceeding the possibility of experimental studies. For doing theoretical research in awide range under the above given criteria it is recommended to use a three-dimensional model only in those cases subjected by significant boundary effects. That means extremly small sliding systems with ahigh length to width ratio as for instance in sliding problems concerning rotary vane and Wankel compressors.

The given experimental results and the possibility to simulate the lubrication conditions mathematically must be used for an analysis of similarity laws. A commonly used method is to describe lubricatio conditions by dimensionless coefficients. For the lubrication conditions of the piston ring Neale /13/ recommends an analysis method given by the Stribeck diagram. Vogelpohl /17/ describes the characteristic evidence of the Stribeck diagram for all kinds of sliding bearings. The minimal lubricating film thickness are to be plotted versus the load factor.

$$LF = \frac{\eta \cdot U}{p_N \cdot RL} \qquad (22)$$

If this coefficient of similarity is relevant for the lubrication conditions of piston, piston ring and liner, all resulting data produced by experiments must form a well-defined interrelation described by a characteristic graph. First the coefficient of friction μ

$$\mu = \frac{F_R}{p_N \cdot A_R} \qquad (23)$$

is treated. It is composed by the ratio of frictional force F_R and the product of specific load p_N normal to the sliding surface and the effective rubbing area A_R. In figure 20 the measured values are composed in this way. As a significant result the characteristic proportionality

$$\mu \sim \frac{\eta \cdot U}{p_N \cdot RL} \qquad (24)$$

for hydrodynamic lubrication is gained by the graph. This functional relationship corresponds to the right hand part of the Stribeck diagram. Also the minimum oil film thickness normalized to c_{min}/RL is plotted versus the coefficient of load. Figure 21 shows the expected tendency published by Neale /13/ which in addition is confirmed by Brown and Hamilton /8/.

The load factor presented here is therefore principally suitable to characterize lubrication conditions in the system of piston, piston ring and cylinder.

CONCLUSIONS

The interacting hydrodynamic unit of piston, piston ring and liner with common lubricating film /1/ is experimentally prooved. For a typical example mathematical and experimental simulation of steady state lubrication conditions have been compared. There exists a good correlationship between theoretical and experimental data. Respecting the effects of finite bearing width lubrication conditions especially for parameter studies can be described by the two-dimensional computer modell. The transformation of measured and calculated data by means of similarity coefficients is advisable. In contrary to the common applicated theory of slider bearings under extremly low loading conditions cavitational phenomena may occur. For the relevant range of working condtions this effect may be neglected.

REFERENCES

/1/ Kruse,H.
Dissertation TH Hannover,1964

/2/ Kruse,H.
MTZ, 1964

/3/ Kruse,H.
Purdue Compr. Techn. Conf.1974

/4/ Burmeister,J.
Dissertation tu Hannover, 1973

/5/ Das,P.K.
SAE Paper 76008, 1976

/6/ Stanton,T.E
The Engineer, 1925

/7/ Stribeck,R.
ZVDI, 1902

/8/ Brown,S.R. Hamilton,G.M.
Jour. Mech. Eng. Sc., 1977

/9/ Schlichting,H.
Grenzschichttheorie, Braun Karlsruhe, 1965

/10/ Kahlert,W.
Ingenieurarchiv, 1948

/11/ Ryk,G.M. Rogov,F.M.
Drigateli vnufrenego sgoranija, 1976

/12/ Englisc,C.
Kolbenringe, Springer Wien, 1960

/13/ Neale,M.J.
Piston ring design, Report TRD 162, 1974

/14/ Braendel,G.
Revue M. Tijdschrift, 1971

/15/ Elson,P.E. Soedel,W.
Purdue Compr. Techn. Conf., 1972

/16/ Wing,R.D. Saunders,O.
Proc. I.M.E., 1972

/17/ Vogelpohl,G.
ZVDI 1954

Fig. 1

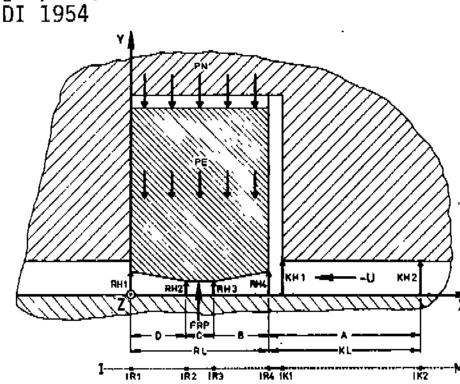

Fig. 2

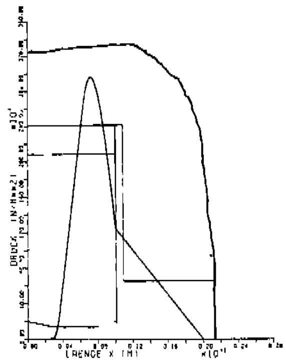

Fig. 3

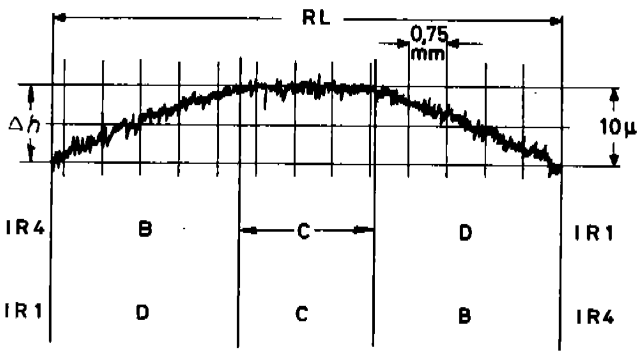

Fig. 5

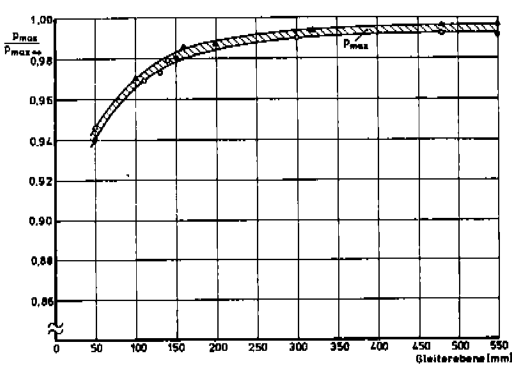

Fig. 6

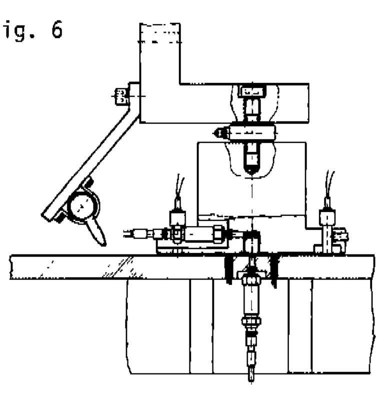

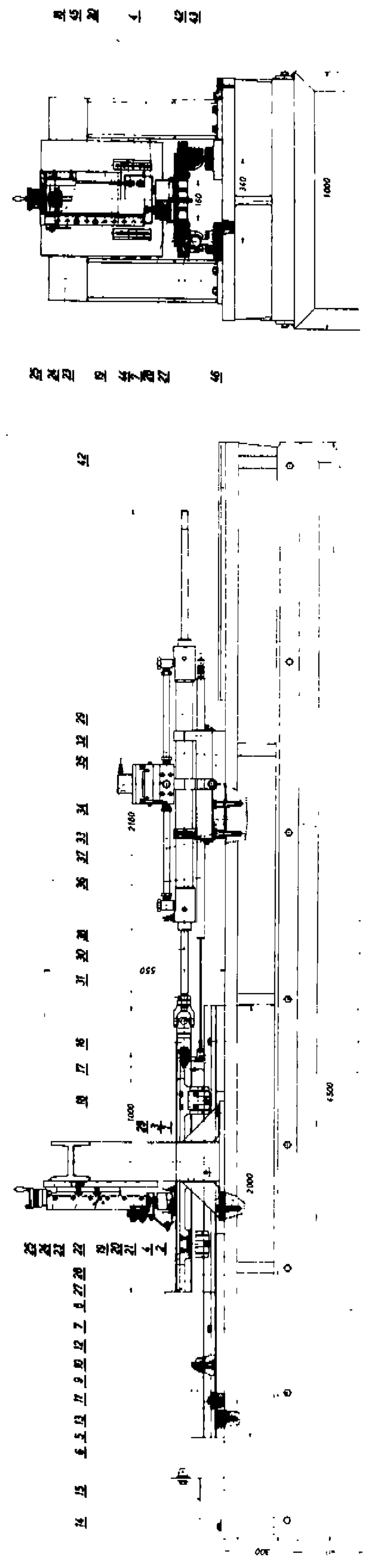

Fig. 4

Fig. 7

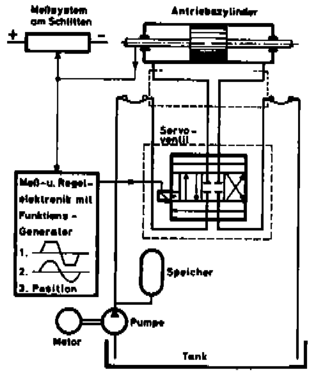

Fig. 11

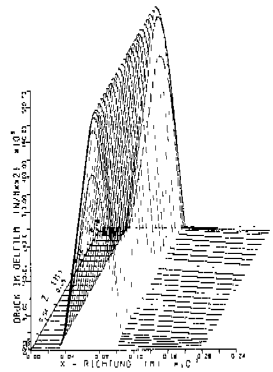

Fig. 12

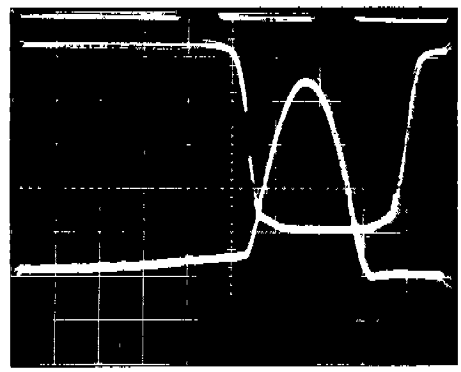

Fig. 8

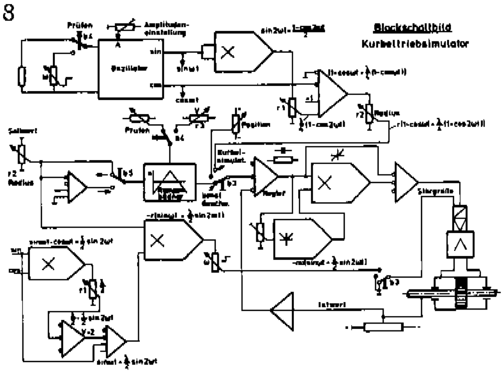

Fig. 9

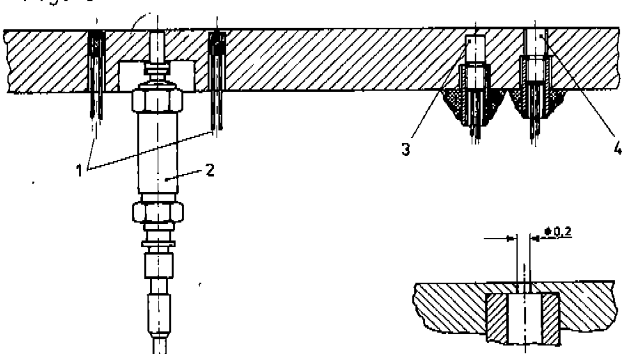

Fig.13

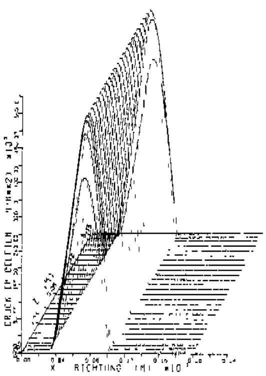

Fig. 10

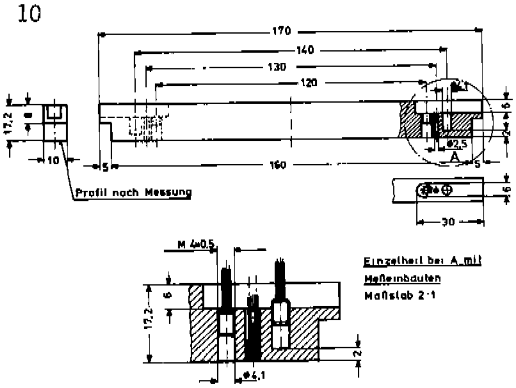

Fig. 14

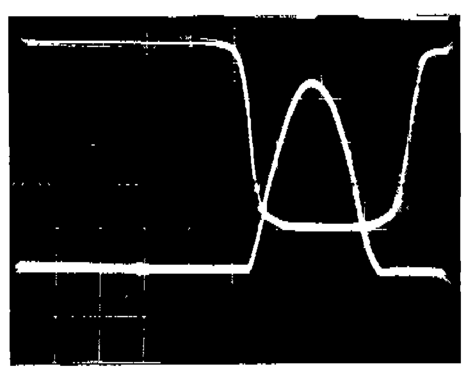

Fig. 15

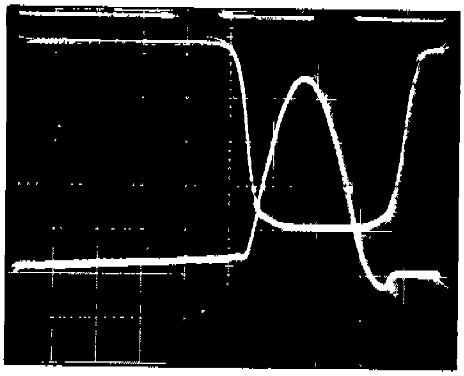

Fig. 19

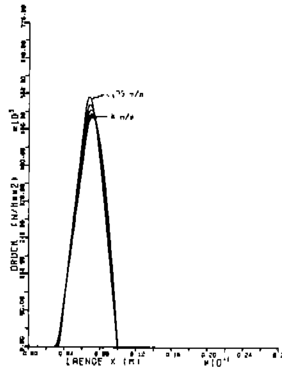

Fig. 16

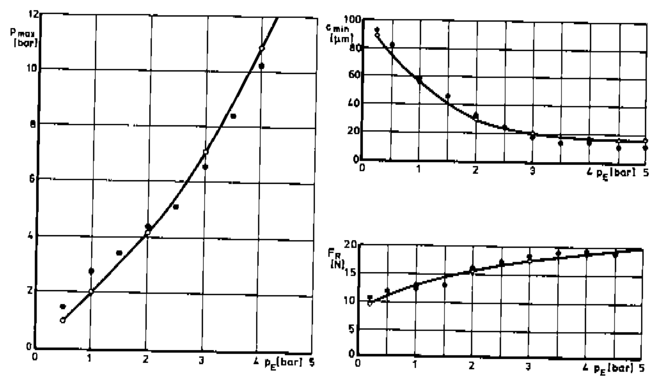

Fig. 20

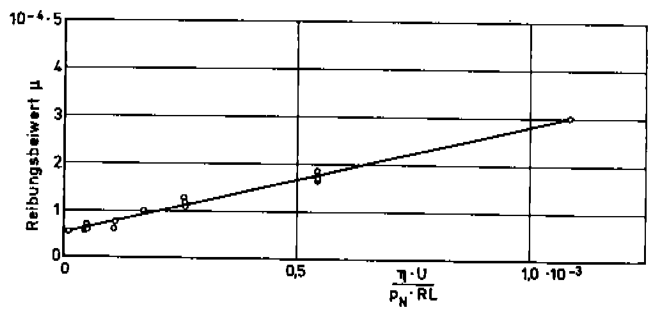

Fig. 17

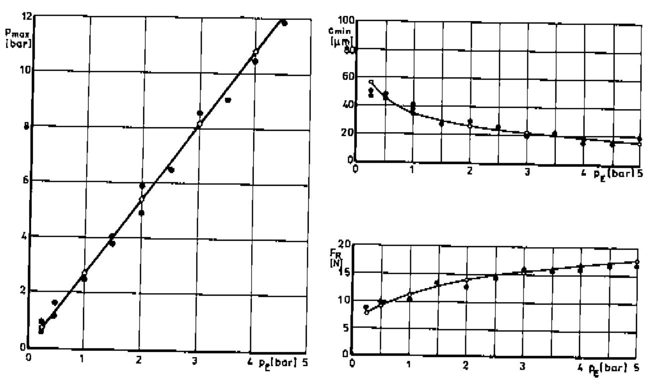

Fig. 21

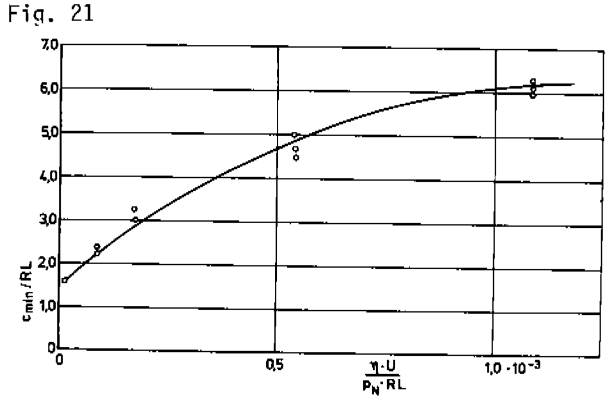

Fig. 18